

# Power Factor Improvement of Bridgeless Isolated Cuk Converter-Fed Brushless DC Motor Drive Using Fuzzy Controller

Mrs. C. BHARATHI

Assistant Professor

Department of Electrical & Electronics Engineering,

GIITS Engineering College, Aganampudi;

Visakhapatnam (Dt); A.P, India.

Email:chamarthibharathi@gmail.com

MS. P .LAVANYA

Assistant Professor

Department of Electrical & Electronics Engineering,

GIITS Engineering College, Aganampudi;

Visakhapatnam (Dt); A.P, India.

Email:plavanya38@gmail.com

**Abstract-**In this paper a Power Factor Correction Cuk converter fed Brushless DC Motor Drive using a Fuzzy Logic Controller is used. The Speed of the Brushless dc motor is controlled by varying the output of the DC capacitor. A Diode Bridge Rectifier followed by a Cuk converter is fed into a Brushless DC Motor to attain the maximum Power Factor. Here we are evaluating the three modes of operation in discontinuous mode and choosing the best method to achieve maximum Power Factor and to minimize the Total Harmonic Distortion. An approach of speed control of the BLDC motor by controlling the dc link voltage of the voltage source inverter (VSI) is used with a single voltage sensor. This facilitates the operation of VSI at fundamental frequency switching by using the electronic commutation of the BLDC motor which offers reduced switching losses. Therefore, the BLDC motor is electronically commutated such that the VSI operates in fundamental frequency switching for reduced switching losses. Moreover, the bridgeless configuration of the CSC converter offers low conduction losses due to partial elimination of diode bridge rectifier at the front end. The proposed configuration shows a considerable increase in efficiency as compared with the conventional scheme. The motor speed control is implemented using fuzzy logic controller. The proposed method is simulated in MATLAB/Simulink with PID and fuzzy logic controller for precise speed control.

**Index Terms**—Bridgeless isolated Cuk converter, brushless dc (BLDC) motor, discontinuous inductor current mode (DICM), power factor correction (PFC), power quality, voltage-source inverter (VSI).

## I. INTRODUCTION

Brushless Dc Motor is recommended for many low cost applications such as household application, industrial, radio controlled cars, positioning and aeromodelling, Heating and ventilation etc. , because of its certain characteristics including high efficiency, high torque to weight ratio, more torque per watt , increased reliability, reduced noise, longer life, elimination of ionizing sparks from the commutator, and overall reduction of electromagnetic interference(EMI) etc. With no windings on the rotor, they are not subjected to any centrifugal forces, and because the windings are supported by the housing, they can be cooled by conduction, requiring no airflow inside the motor for cooling purposes. The motor's internals can be entirely enclosed and protected from dust, dirt or any other foreign obstacles.

The two main factors that determine the power quality of a motor are the Power Factor (PF) and the total harmonic Distortion (THD) [1]. The Power Factor determines the amount of useful power being consumed by an electrical system. The term THD is defined as the ratio of the harmonic components of voltage (or current) to the voltage (or current) of the fundamental. So the Power Factor Correction (PFC) is the best method of improving the PF by making the [2-3] input to the power supply purely resistive or else due to the presence of non linear loads the input will contain phase displacement which causes harmonic distortion and thus the power factor gets degraded.

The selection of mode of operation is a tradeoff between the allowed stresses on PFC switch and cost of the around system during the operating mode of front-end converter. The two different modes of operation are depending on design parameters; either continuous or discontinuous conduction mode approach may lead the converter. In this design, a BLDC motor drive fed by a PFC BL-Cuk converter operates in four modes [4]. At the time of starting or overloading inrush current is created. The inrush current occurring at start-up or overload was eliminated by operating the PFC in discontinuous conduction mode (DCM), it also gives natural protection for switches, low input ripple, and less electromagnetic interference (EMI) [5]. In this paper a fuzzy controlled BL- Cuk converter is analyzed in terms of harmonic reduction.

A conventional PFC Cuk [6-7] rectifier is shown in fig 1. The current flows through two rectifier bridge diodes and the power switch (Q) during the switch ON-time, and through two rectifier bridge diodes and the output diodes (D0) during the switch OFF- time. During each switching cycle, the current flows through three semiconductor devices. As a result, a significant conduction loss, caused by the forward voltage drop across the bridge diode. In a bridgeless PFC circuits [8], where the number of semiconductors generating losses will be reduced by eliminating the full bridge input diode rectifier. A bridgeless PFC rectifier allows the current to flow through a minimum number of switching devices compared to the conventional Cuk rectifier [9]. It also reduces the converter conduction losses and which improves the efficiency and reducing the cost. A bridgeless power factor correction rectifier

is introduced to improve the rectifier power density and/or to reduce noise emission via soft-switching techniques or coupled magnetic topologies. The Cuk converter has several advantages in power factor correction application [10] ns, such as easy implementation of transformer isolation, natural protection against inrush current occurring at start-up or overload current, lower input current ripple, and less electromagnetic interference(EMI) associated with discontinuous conduction mode topology.

A BLDC motor when fed by a diode bridge rectifier [11] (DBR) has higher conduction losses. The high conduction loss caused by the high forward voltage drop of the bridge diode begins to degrade the overall system efficiency. The heat generated within the bridge rectifier may destroy the individual diodes. Hence, it becomes necessary to utilize a bridge rectifier with higher current handling capability or heat dissipating characteristics. This increases the size and cost of the power supply, which is unacceptable for an efficient design. Bridgeless topologies seem to be the best solution for reducing the conduction and switching losses of the converter.

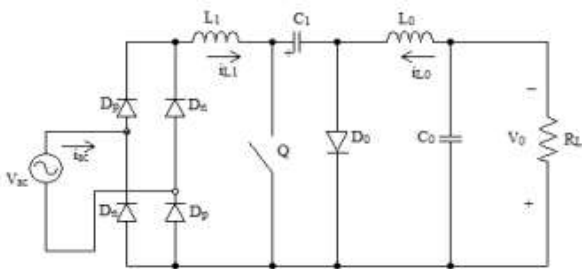


Fig.1 Conventional Cuk Rectifier

## II. Operation of PFC Based Bridgeless Isolated CUK Converter

The operation of the proposed PFC converter is classified into two different sections for a line cycle and a switching cycle. Fig.2 shows six different modes of operation. Moreover, Fig.3 shows the associated waveforms of the PFC converter during a complete switching period.

### A. Operation during Complete Line Cycle of Supply Voltage

The proposed bridgeless isolated Cuk converter is designed such that switches  $S_{w1}$  and  $S_{w2}$  conduct for positive and negative half cycles of supply voltage, respectively.

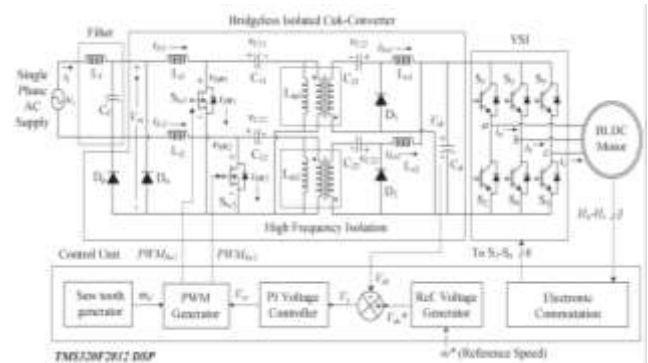
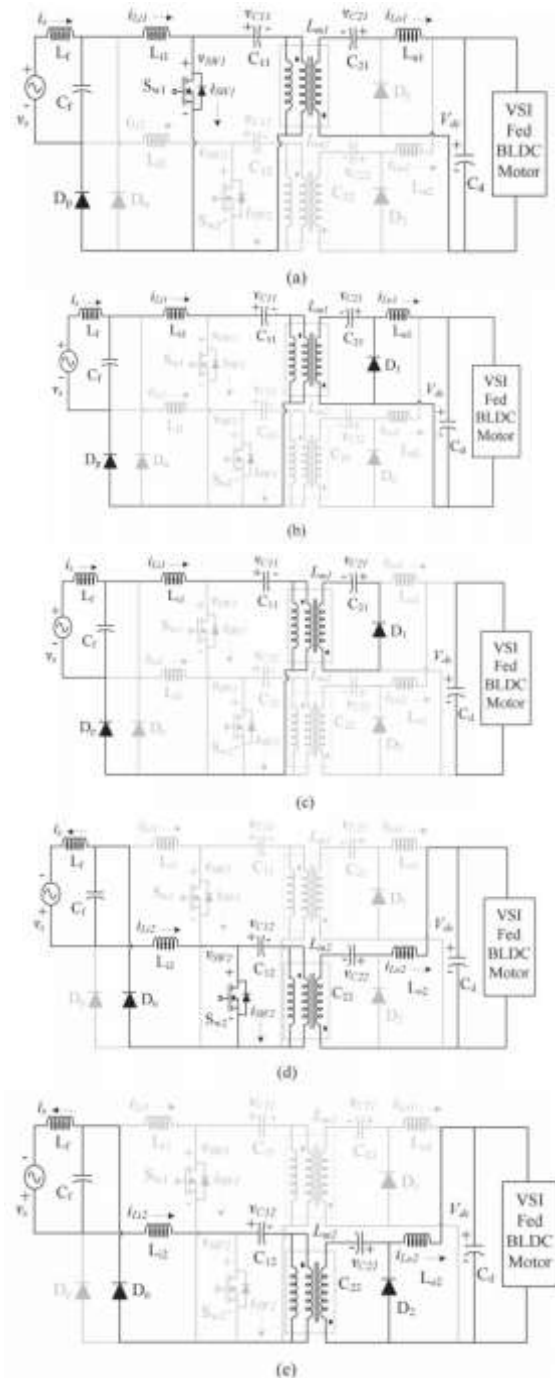


Fig.2. Proposed configuration of a bridgeless isolated Cuk converter-fed BLDC motor drive.



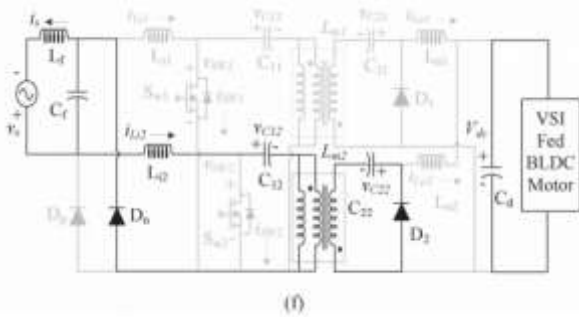


Fig.3. Different modes of operation of bridgeless isolated Cuk converter during (a)–(c) positive and (d)–(f) negative half cycle of supply voltage.

During the positive half cycle of supply voltage, switch  $S_{w1}$ , inductors  $L_{i1}$  and  $L_{o1}$ , intermediate capacitors  $C_{11}$  and  $C_{21}$ , and diodes  $D_1$  and  $D_p$  are in the state of conduction and vice versa for the negative half cycle of supply voltage as shown in Fig.3(a)–(f). As shown in these figures, the proposed PFC converter operates in three different modes during the positive and negative half cycles of the supply voltage. Moreover, during the DICM operation, the current of output inductors ( $L_{o1}$  and  $L_{o2}$ ) become discontinuous in a switching period.

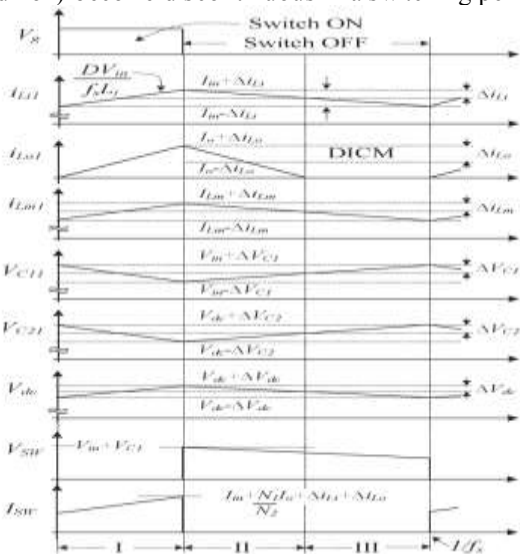


Fig.4. Waveforms of proposed converter in complete switching cycle. However, the current flowing in the input and magnetizing inductance of the high frequency transformer (HFT) ( $L_{i1}$ ,  $L_{i2}$ ,  $L_{m1}$ , and  $L_{m2}$ ) and the voltage across the intermediate capacitor ( $C_{11}$ ,  $C_{12}$ ,  $C_{21}$ , and  $C_{22}$ ) remain continuous in a complete switching period.

### III. Operation during Complete Switching Cycle

Fig.3(a)–(c) shows three modes of operation of a bridgeless isolated Cuk converter in a switching period for the positive half cycle of the supply voltage. Fig.3 shows its associated waveforms in DICM ( $L_o$ ) mode of operation as follows.

**Mode P-I:** In this mode, when the switch ( $S_{w1}$ ) is turned on, the input inductor ( $L_{i1}$ ), output inductor ( $L_{o1}$ ), and magnetizing inductance of HFT ( $L_{m1}$ ) start charging as shown in Fig.3(a). The input side

intermediate capacitor ( $C_{11}$ ) supplies the energy to the HFT, and the output side intermediate capacitor ( $C_{21}$ ) supplies the required energy to the dc link capacitor as shown in Fig.3.

**Mode P-II:** When the switch ( $S_{w1}$ ) is turned off, the input inductor ( $L_{i1}$ ), output inductor ( $L_{o1}$ ), and magnetizing inductance of HFT ( $L_{m1}$ ) start discharging as shown in Fig.3(b). The intermediate capacitors ( $C_{11}$  and  $C_{21}$ ) charge, and the dc link capacitor ( $C_d$ ) discharges in this interval as shown in Fig.4.

**Mode P-III:** During this interval, the output side inductor ( $L_{o1}$ ) is completely discharged, and the input inductor ( $L_{i1}$ ) and magnetizing inductance of HFT ( $L_{m1}$ ) continue to discharge as shown in Fig.3(c).

The output side intermediate capacitor ( $C_{21}$ ) continues to charge, and the dc link capacitor ( $C_d$ ) supplies the required energy to the BLDC motor (BLDCM) as shown in Fig.4.

In a similar way, the operation for the negative half cycle of the supply voltage is realized. Initially, the intermediate capacitors ( $C_{11}$ ,  $C_{12}$ ,  $C_{21}$ , and  $C_{22}$ ) are completely discharged and are charged during the operation of the PFC converter. The voltage across the input side intermediate capacitors ( $C_{11}$  and  $C_{12}$ ) depends upon the instantaneous input voltage; hence, the initial charging of  $C_{11}$  and  $C_{12}$  is zero. However, the output side intermediate capacitors ( $C_{21}$  and  $C_{22}$ ) are not completely discharged in a switching period or a half line cycle of the supply voltage due to the voltage maintained at the dc link capacitor ( $C_d$ ).

Moreover, during the operation of the PFC converter in the positive half cycle, the energy storage components on the primary side of the HFT (i.e.,  $L_{i2}$ ,  $C_{12}$  and  $L_{m2}$ ) remain in non-conducting state and are completely discharged. However, the energy storage components on the secondary side of HFT (i.e.,  $C_{22}$ ) remain charged at its full voltage due to the unavailability of a discharging path and the presence of the dc link capacitor ( $C_d$ ).

### IV. DESIGN OF BRIDGELESS ISOLATED CUK CONVERTER

A bridgeless isolated Cuk converter is designed to operate in DICM such that the current flowing in the output inductors ( $L_{o1}$  and  $L_{o2}$ ) becomes discontinuous in a switching period. A PFC converter of 250 W ( $P_{max}$ ) is designed for the selected BLDC motor (specifications given in the Appendix). For a wide range of speed, the dc link voltage is controlled from 50 V ( $V_{dmin}$ ) to a rated voltage of 130 V ( $V_{dmax}$ ) with a supply voltage variation from 170 V ( $V_{smin}$ ) to 270 V ( $V_{smax}$ ). The input voltage  $v_s$  applied to the PFC converter is given as

$$v_s(t) = V_m \sin(2\pi f_L t) = 220\sqrt{2} \sin(314t) \quad (1)$$

Where  $V_m$  is the peak input voltage (i.e.,  $\sqrt{2}V_S$ ) and  $f_L$  is the line frequency, i.e., 50 Hz.

Now, the instantaneous value of the rectified voltage is given as

$$V_{in}(t) = |V_m \sin(\omega t)| = |220\sqrt{2} \sin(314t)| \quad (2)$$

Where  $||$  represents the modulus function.

The output voltage  $V_{dc}$  of a bridgeless isolated Cuk converter which is a buck-boost configuration is given as

$$V_{dc} = \left(\frac{N_2}{N_1}\right) \frac{D}{(1-D)} V_{in} \quad (3)$$

Where  $D$  represents the duty ratio and  $(N_2/N_1)$  is the turn's ratio of the HFT which is taken as 1/2 for this application. The instantaneous value of the duty ratio,  $D(t)$ , depends on the input voltage and dc link voltage. Instantaneous duty ratio  $D(t)$  is obtained by substituting (2) in (3) as follows:

$$D(t) = \frac{V_{dc}}{(N_2/N_1)V_{in}(t) + V_{dc}} = \frac{V_{dc}}{(N_2/N_1)|V_m \sin(\omega t)| + V_{dc}} \quad (4)$$

Since the speed of the BLDC motor is controlled by varying the dc link voltage of VSI, therefore, the instantaneous power  $P_i$  is taken as a linear function of  $V_{dc}$  as follows:

$$P_i = \left(\frac{P_{max}}{V_{dcmax}}\right) V_{dc} \quad (5)$$

Where  $V_{dcmax}$  represents the maximum dc link voltage and  $P_{max}$  is the rated power of the PFC converter. Using (5), the minimum power at the minimum dc link voltage of 50 V ( $V_{dcmin}$ ) is calculated as 96 W ( $P_{min}$ ). The value of the input inductor to operate in continuous conduction is decided by the amount of permitted ripple current ( $\eta$ ) and is given as [12]

$$L_{i1,2} = \frac{V_{in}(t)D(t)}{\eta I_{in}(t) f_s} = \frac{1}{\eta f_s} \left(\frac{V_s^2}{P_i}\right) \left(\frac{V_{dc}}{nV_{in}(t) + V_{dc}}\right) \quad (6)$$

Where  $f_s$  is the switching frequency which is taken as 20 kHz. The maximum inductor ripple current is obtained at the rated condition, i.e.,  $V_{dcmax}$  ( $P_i = P_{max}$ ) for a minimum value of the supply voltage ( $V_{smin}$ ). Hence, the input side inductor is designed at the peak value of the minimum supply voltage ( $\sqrt{2}V_{smin}$ ).

Using (6), the value of the input side inductors ( $L_{i1}$  and  $L_{i2}$ ) is calculated as 5.005 mH for a permitted current ripple of 50% ( $\eta$ ) of the input current. Hence, the input side inductor of 5 mH is selected for its operation in continuous conduction. The critical value of the output side inductor ( $L_{oc}$ ) to operate at the boundary of CICM and DICM is given as [12]

$$L_{oc} = \frac{V_{dc} \{1-D(t)\}}{2I_{Lo}(t) f_s} = \frac{V_{dc} D(t)}{2I_{in}(t) f_s} \\ = \frac{R_{in} V_{dc} D(t)}{2V_{in}(t) f_s} = \left(\frac{V_s^2}{P_i}\right) \frac{V_{dc}}{2V_{in}(t) f_s} \left(\frac{V_{dc}}{nV_{in}(t) + V_{dc}}\right) \quad (7)$$

The maximum current ripple in an inductor occurs at the maximum power and at the minimum value of the supply voltage (i.e.,  $V_{smin}$ ). Hence, the output inductor is calculated at the peak of the supply voltage (i.e.,  $V_{in} = \sqrt{2}V_{smin}$ ).

The critical value of output side inductors is calculated at the minimum ( $L_{oc50}$ ) and maximum ( $L_{oc130}$ ) values of dc link voltages using (7) as 459.79 and 811.93  $\mu$ H, respectively. Hence, the critical value of the output inductor is selected lower than the minimum value, i.e.,  $L_{oc50}$ , to ensure a discontinuous conduction even at lower values of dc link voltages. Therefore, the output inductor ( $L_{o1}$  and  $L_{o2}$ ) of 70  $\mu$ H is selected for its operation in discontinuous conduction. The value of the magnetizing inductance of HFT to operate in CICM is decided by the permitted ripple current ( $\xi$ ) as [11]

$$L_{m1,2} = \frac{V_{dc} \{1-D(t)\}}{\Delta I_{Lm}(t) n f_s} = \left(\frac{V_s^2}{P_i}\right) \frac{1}{\xi f_s} \left(\frac{V_{dc}}{nV_{in}(t) + V_{dc}}\right) \quad (8)$$

The maximum current occurs at the maximum dc link voltage (i.e.,  $P_{max}$ ) and the minimum supply voltage (i.e.,  $V_{smin}$ ). Therefore, the value of the magnetizing inductance ( $L_{m1}$  and  $L_{m2}$ ) for a permitted ripple current ( $\xi$ ) of 50% is calculated using (8) as 6.006 mH and is selected as 6 mH. The value of input side intermediate capacitors to operate in CCM with a permitted ripple voltage of  $\kappa\%$  of  $V_{C1}$  is given as [11]

$$C_{11,12} = \frac{V_{in} n^2 \{D(t)\}^2}{\Delta V_{C1}(t) R_L f_s \{1-D(t)\}} \\ = \frac{n P_i}{\kappa (\sqrt{2} V_s) f_s (n\sqrt{2} V_s + V_{dc})} \quad (9)$$

The input side intermediate capacitors ( $C_{11}$  and  $C_{12}$ ) are calculated at the maximum value of voltage ripple corresponding to the maximum supply voltage ( $V_{smax}$ ) and at rated dc link voltage. Now, for a permitted ripple voltage of 25%, the values of  $C_{11}$  and  $C_{12}$  are calculated using (9) as 204 nF and are selected as 220 nF.

The value of output side intermediate capacitors to operate in CCM with a permitted ripple voltage of  $\chi\%$  of  $V_{C2}$  is given as [11]

$$C_{21,22} = \frac{V_{dc} D(t)}{\Delta V_{C2}(t) R_L f_s} = \frac{P_i}{\chi V_{dc} f_s (n\sqrt{2} V_s + V_{dc})} \quad (10)$$

Now, the maximum ripple voltage occurs at rated condition and at the maximum value of dc link voltage ( $V_{dcmax}$ ). Hence, the output side intermediate capacitor ( $C_d$ ) is calculated at the maximum permitted ripple voltage of 10% ( $\chi$ ) of  $V_{C21,22}$  at the maximum ( $C_{2c270}$ ) and minimum ( $C_{2c170}$ ) values of supply voltage as 2.99 and 3.84  $\mu$ F, respectively. Therefore, the output side intermediate capacitors ( $C_{21}$  and  $C_{22}$ ) are selected higher than  $C_{2c85}$  of the order of 4.4  $\mu$ F.

The value of the dc link capacitor ( $C_d$ ) is calculated as [11]

$$C_d = \frac{I_{dc}}{2\omega \Delta V_{dc}} = \left(\frac{P_i}{V_{dc}}\right) \frac{1}{2\omega (\rho V_{dc})} \quad (11)$$

Where  $\Delta V_{dc}$  represents the permitted ripple in the dc link voltage.

The worst case design occurs for the minimum value of dc link voltage, i.e., 50 V. Hence, for a permitted ripple voltage of 3% ( $\rho$ ), the value of the dc link capacitor is calculated using (11) as 2038  $\mu$ F, and it is selected as 2200  $\mu$ F.

A low-pass LC filter is used to avoid the reflection of higher order harmonics in the supply system. The maximum value of the filter capacitance ( $C_{max}$ ) is given as [40]

$$C_{max} = \frac{I_m}{\omega_L V_m} \tan(\theta) = \frac{(P_{max} \sqrt{2}/V_s)}{\omega_L \sqrt{2} V_s} \tan(\theta) \quad (12)$$

Where  $\theta$  is the displacement angle between the fundamental value of the supply voltage and supply current and is taken as  $2^\circ$ .

The maximum value of the filter capacitor is calculated using (12) as 574.4 nF and is selected as 330 nF. The value of the filter inductor is designed by considering the source impedance ( $L_s$ ) of 4%–5% of the base impedance. Hence, the additional value of inductance required is given as

$$L_f = L_{req} + L_s \Rightarrow L_{req} = L_f - L_s$$

$$L_{req} = \frac{1}{4\pi^2 f_c^2 C_f} - 0.025 \left( \frac{1}{\omega_L} \right) \left( \frac{V_s^2}{P_o} \right) \quad (13)$$

Where  $f_c$  is the cutoff frequency which is selected such that  $f_L < f_c < f_s$ . Therefore,  $f_c$  is taken as  $f_s/10$ . Hence; the value of the filter inductance is calculated using (13) as 3.77 mH.

### V. Control of PFC Bridgeless Isolated CUK Converter-Fed BLDC Motor Drive

The control of the proposed BLDC motor drive is divided into two categories of control of the PFC converter for dc link voltage control and control of three-phase VSI for achieving the electronic commutation of the BLDC motor as follows.

#### A. Control of Front-End PFC Converter

A voltage follower approach is used for the control of the PFC-based bridgeless isolated Cuk converter operating in DICM. This control scheme consists of a reference voltage generator, a voltage error generator, a voltage controller, and a PWM generator. A “Reference Voltage Generator” generates a reference voltage  $V^*_{dc}$  by multiplying the reference speed ( $\omega^*$ ) with the motor’s voltage constant ( $k_v$ ) as

$$V_{dc}^* = k_v \omega^* \quad (14)$$

The “Voltage Error Generator” compares this reference dc link voltage ( $V^*_{dc}$ ) with the sensed dc link voltage ( $V_{dc}$ ) to generate an error voltage ( $V_e$ ) given as

$$V_e(k) = V_{dc}(k) - V_{dc}^*(k) \quad (15)$$

Where “k” represents the kth sampling instance. This error voltage  $V_e$  is given to a voltage proportional

integral (PI) controller to generate a controlled output voltage ( $V_{cc}$ ) which is expressed as

$$V_{cc}(k) = V_{cc}(k-1) + K_p \{V_e(k) - V_e(k-1)\} + K_i V_e(k) \quad (16)$$

Finally, the PWM signals for switches Sw1 and Sw2 are generated by comparing the output of the PI controller ( $V_{cc}$ ) with the high-frequency saw tooth signal ( $m_d$ ) given as

$$\text{For } V_S > 0; \begin{cases} \text{if } m_d < V_{cc} \text{ then } PWM_{Sw1} = 'ON' \\ \text{if } m_d \geq V_{cc} \text{ then } PWM_{Sw1} = 'OFF' \end{cases}$$

$$\text{For } V_S < 0; \begin{cases} \text{if } m_d < V_{cc} \text{ then } PWM_{Sw2} = 'ON' \\ \text{if } m_d \geq V_{cc} \text{ then } PWM_{Sw2} = 'OFF' \end{cases} \quad (17)$$

Where  $PWMSw1$  and  $PWMSw2$  represent the gate signals to PFC converter switches Sw1 and Sw2, respectively.

In this control algorithm, (17) shows the solid-state switches of the PFC converter operating at half cycles of supply voltages. However, to avoid the sensing of supply voltage for zero crossing detection, only one PWM signal is generated to drive both solid-state switches of the PFC converter, i.e.,  $PWMSw1 = PWMSw2$ . Moreover, the PFC converter is operating in DCM; therefore, the input current shaping in phase with the supply voltage is obtained inherently, and a unity PF is achieved at the ac mains.

#### B. Control of BLDC Motor Electronic Commutation

An electronic commutation of the BLDC motor includes the proper switching of the VSI in such a way that a symmetrical dc current is drawn from the dc link capacitor for  $120^\circ$  and is placed symmetrically at the center of the back electro-motive force (EMF) of each phase. A Hall-effect position sensor is used to sense the rotor position on a span of  $60^\circ$ ; which is required for the electronic commutation of the BLDC motor. As shown in Fig. 4, when two switches of the VSI, i.e., S1 and S4, are in conducting states, a line current  $i_{ab}$  is drawn from the dc link capacitor whose magnitude depends on the applied dc link voltage ( $V_{dc}$ ), back EMFs ( $e_{an}$  and  $e_{bn}$ ), resistances ( $R_a$  and  $R_b$ ), and self-inductance and mutual inductance ( $L_a$ ,  $L_b$ , and  $M$ ) of stator windings. This current produces an electromagnetic torque ( $T_e$ ) which, in turn, increases the speed of the BLDC motor.

### VI. INTRODUCTION TO FUZZY LOGIC CONTROLLER

L. A. Zadeh presented the first paper on fuzzy set theory in 1965. Since then, a new language was developed to describe the fuzzy properties of reality, which are very difficult and sometime even impossible to be described using conventional methods. Fuzzy set theory has been widely used in the control area with some application to dc-to-dc converter system. A simple fuzzy logic control is built up by a group of rules based on the human knowledge of system behavior. Matlab/Simulink simulation model is built to study the dynamic behavior of dc-to-dc converter and

performance of proposed controllers. Furthermore, design of fuzzy logic controller can provide desirable both small signal and large signal dynamic performance at same time, which is not possible with linear control technique. Thus, fuzzy logic controller has been potential ability to improve the robustness of dc-to-dc converters. The basic scheme of a fuzzy logic controller is shown in Fig 6 and consists of four principal components such as: a fuzzification interface, which converts input data into suitable linguistic values; a knowledge base, which consists of a data base with the necessary linguistic definitions and the control rule set; a decision-making logic which, simulating a human decision process, infer the fuzzy control action from the knowledge of the control rules and linguistic variable definitions; a de-fuzzification interface which yields non fuzzy control action from an inferred fuzzy control action [10].

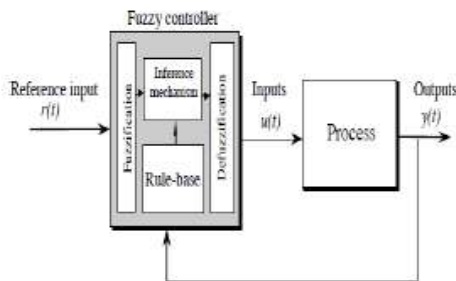


Fig.5. General Structure of the fuzzy logic controller on closed-loop system

The fuzzy control systems are based on expert knowledge that converts the human linguistic concepts into an automatic control strategy without any complicated mathematical model [10]. Simulation is performed in buck converter to verify the proposed fuzzy logic controllers.

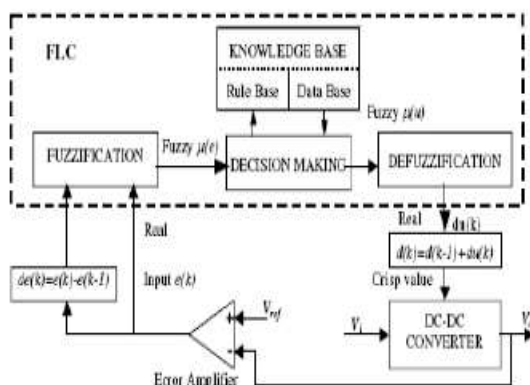
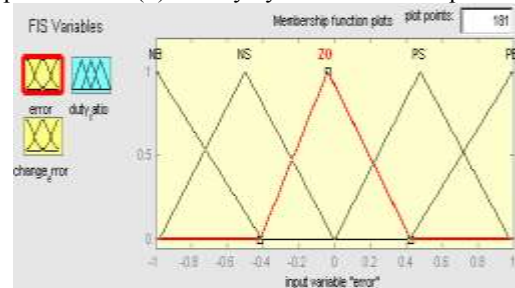


Fig.6. Block diagram of the Fuzzy Logic Controller (FLC) for dc-dc converters

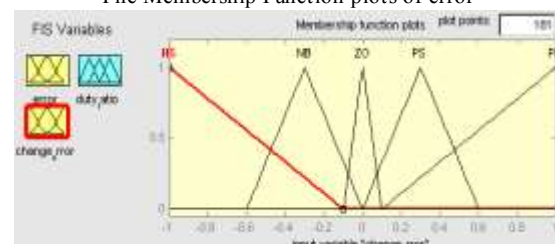
**A. Fuzzy Logic Membership Functions:**

The dc-dc converter is a nonlinear function of the duty cycle because of the small signal model and its control method was applied to the control of boost converters. Fuzzy controllers do not require an exact mathematical model. Instead, they are designed based on general knowledge of the plant. Fuzzy controllers are designed

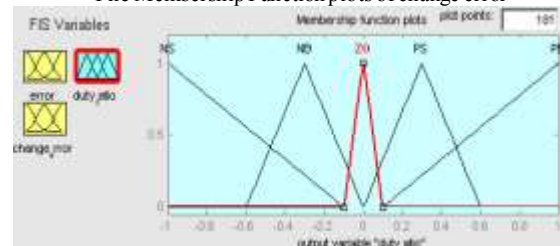
to adapt to varying operating points. Fuzzy Logic Controller is designed to control the output of boost dc converter using Mamdani style fuzzy inference system. Two input variables, error (e) and change of error (de) are used in this fuzzy logic system. The single output variable (u) is duty cycle of PWM output.



The Membership Function plots of error



The Membership Function plots of change error



The Membership Function plots of duty ratio

**B. Fuzzy Logic Rules:**

The objective of this dissertation is to control the output voltage of the boost converter. The error and change of error of the output voltage will be the inputs of fuzzy logic controller. These 2 inputs are divided into five groups; NB: Negative Big, NS: Negative Small, ZO: Zero Area, PS: Positive small and PB: Positive Big and its parameter [10]. These fuzzy control rules for error and change of error can be referred in the table that is shown in Table I as per below:

Table I

Table rules for error and change of error

(de) \ (e)	NB	NS	ZO	PS	PB
NB	NB	NB	NB	NS	ZO
NS	NB	NB	NS	ZO	PS
ZO	NB	NS	ZO	PS	PB
PS	NS	ZO	PS	PB	PB
PB	ZO	PS	PB	PB	PB

VII. MATLAB/SIMULATION RESULTS

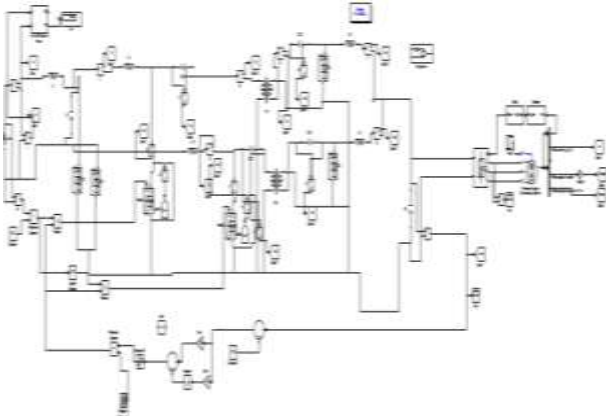


Fig 7 Matlab/simulation circuit of proposed configuration of a bridgeless isolated Cuk converter-fed BLDC motor drive.

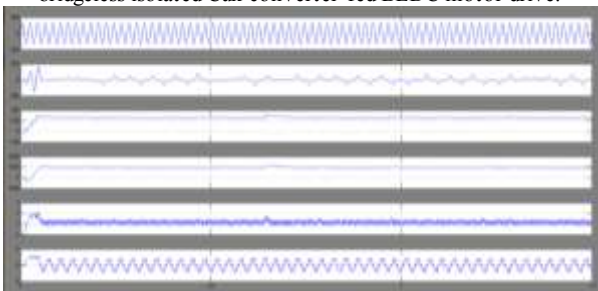


Fig 8 simulation wave form of Test results of the proposed drive during its operation at rated loading condition with dc link voltage as 130 V

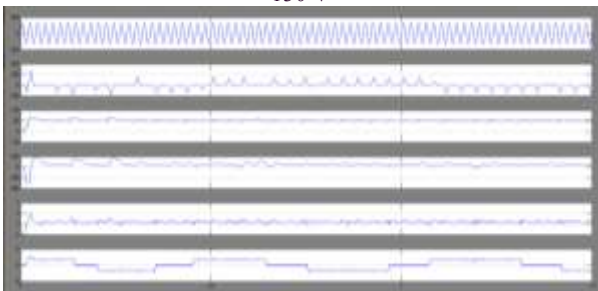


Fig 9 simulation wave form of Test results of the proposed drive during its operation at rated loading condition with dc link voltage as 50 v

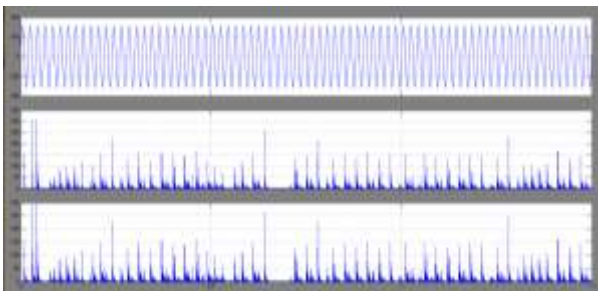


Fig 10 simulation wave form of source voltage

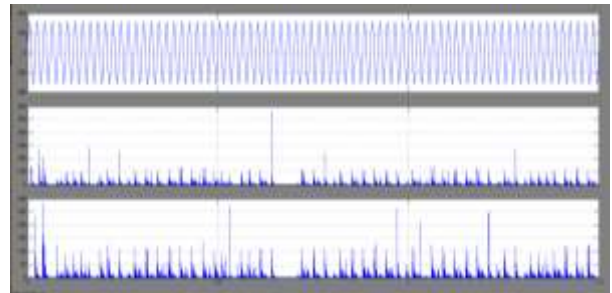


Fig 11 Test results of the proposed drive during its operation at rated condition showing (a) input inductor currents, (b) output inductor currents, and (c) HFT currents

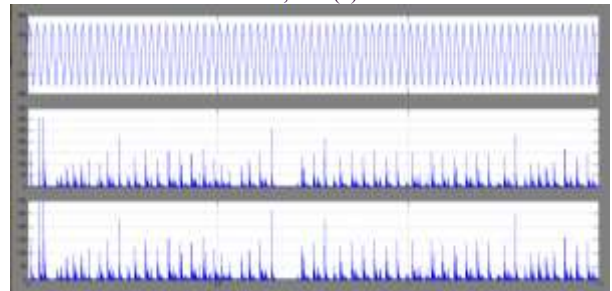


Fig 12 Test results of the proposed drive during its operation at rated condition showing intermediate capacitor voltages (a) VC11 and VC12 and (b) VC21 and VC22.

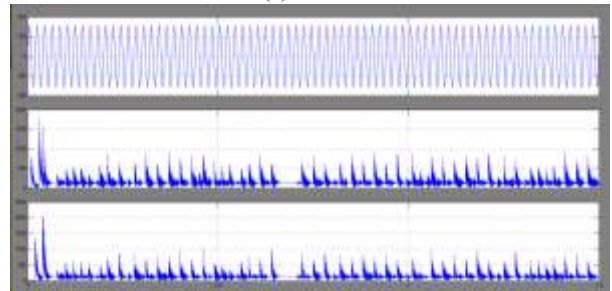
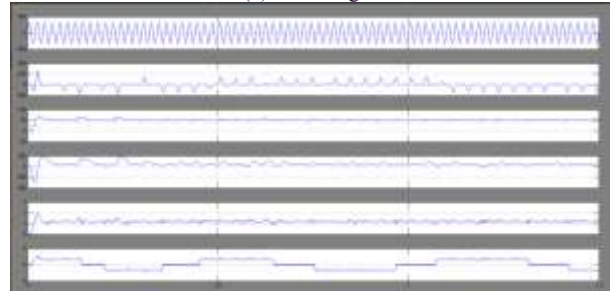
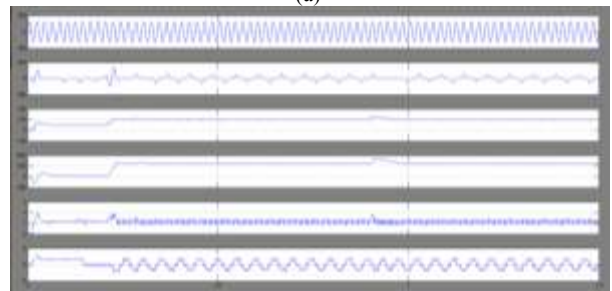


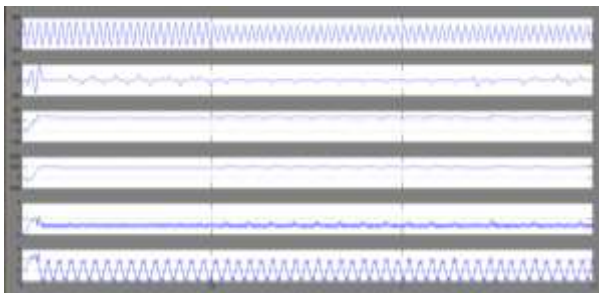
Fig 13 Test results of the proposed drive during its operation at rated condition showing (a) voltage and current stress on PFC converter switches and (b) its enlarged waveforms.



(a)



(b)



(c)

Fig 14 Test results of the proposed drive during (a) starting at dc link voltage of 50 V, (b) speed control corresponding to change in dc link voltage from 50 to 100 V, and (c) supply voltage fluctuation from 250 to 200 V.

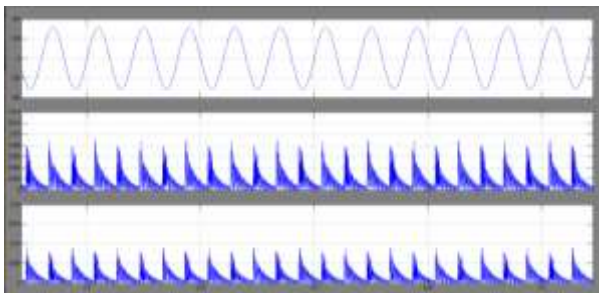


Fig 15 Test results of the proposed drive during its operation at rated condition showing (a) input inductor currents, (b) output inductor currents, and (c) HFT currents with fuzzy logic.

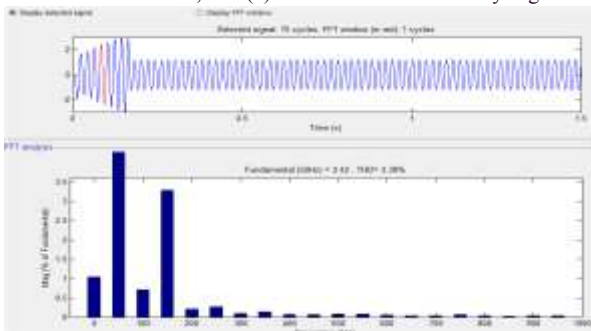


Fig.16.FFT analysis of source current THD with PI Controller.

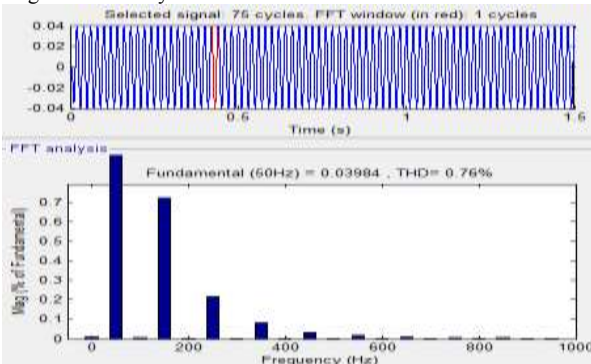


Fig.17. FFT analysis of source current THD with fuzzy logic

### VIII. CONCLUSION

The bridgeless Cuk converter fed BLDC motor drive improves the power factor at the AC mains near to the unity with precise speed control of fuzzy logic controller with low THD. The suitable controller for PFC operation of BLDC motor drives has been analyzed. FLC seems to be the best controller in

performance improvement of BLDC motor drives for attaining the power factor near to unity. The Simulink model for a BLDC Motor drive system with stator current control by using Simulink blocks has been developed and operated at rated speed. A mathematical expression of the system is simply incorporated in the MATLAB simulation and the usage of numerous appliance boxes and support guides simplifies the simulation of large control system. Simulink is effective of recommending real time results with reduced simulation time process and debugging. Usually in such drive system the inverter is driven by Fuzzy Logic controller. The proposed drive system has maintained high power factor and improved power quality for a wide range of speed control for varying supply voltages. The Simulink simulation allows performance study of BLDC Motor drives with DCM. It is found that the power factor is near unity with the use of BL-Cuk converter. The efficiency increases due to the increase in the power factor.

### REFERENCES

- [1] C. L. Xia, Permanent Magnet Brushless DC Motor Drives and Controls. Hoboken, NJ, USA: Wiley, 2012.
- [2] C. L. Xia, Brushless DC Motor Drives and Controls .Beijing, China: Wiley, 2012.
- [3] B. Singh and V. Bist, "An improved power quality bridgeless Cuk converter fed BLDC motor drive for air conditioning system," IET Power Electron., vol. 6, no. 5, pp. 902–913, 2013.
- [4] Pradeep Kumar, P.R.Sharma and Ashok Kumar, "Simulation and design of power factor correction prototype for BLDC motor control," European scientific journal, vol. 9, no. 12, April 2013.
- [5] A. Sabzali, E. H. Ismail, M. Al-Saffar, and A. Fardoun, "New bridgeless DCM sepic and Cuk PFC rectifiers with low conduction and switching losses," IEEE Trans. Ind. Appl., vol. 47, no. 2, pp. 873–881, Mar./Apr.2011.
- [6] G. Moschopoulos and P. Kain, "A novel single-phase soft-switched rectifier with unity power factor and minimal component count," IEEE Trans. Ind. Electron., vol. 51, no. 3, pp. 566–575, Jun. 2004.
- [7] W. Choi, J.Kwon, E. Kim, J. Lee, and B.Kwon, "Bridgeless boost rectifier with low conduction losses and reduced diode reverse-recovery problems," IEEE Trans. Ind. Electron., vol. 54, no. 2, pp. 769–780, Apr.2007.
- [8] E. H. Ismail, "Bridgeless SEPIC rectifier with unity power factor and reduced conduction losses," IEEE Trans. Ind. Electron., vol. 56, no. 4, pp.1147–1157, Apr. 2009.
- [9] Y.-S. Roh, Y.-J. Moon, J.-C. Gong, and C. Yoo, "Active power factor correction (PFC) circuit with resistor-free zero-current detection," IEEE Trans. Power Electron., vol. 26, no. 2, pp. 630–637, Feb. 2011.
- [10] Singh, B., and Bist, V., "Power quality improvement in PFC bridgeless Cuk fed BLDC motor drive", Int. J. Emerg. Elect. Power Syst., Vol. 14, No. 3, PP. 285–296, 2013.
- [11] Bist, V., and Singh, B., "A reduced sensor PFC BL zeta converter based VSI fed BLDC motor drive", Elect. Power Syst. Res, Vol. 98, PP. 11– 18, May 2013.

### AUTHORS:



C. BHARATHI Received her B.Tech Degree from Ranippettai Engineering College, Walaja, Vellore, Tamilnadu and M.Tech from Bharathi University, Chennai. She is currently working as Assistant Professor in Department of EEE, GIITS Engineering college,

Aganampudi, Visakhapatnam (Dt), Andhra Pradesh, India. Her area of Interest is Electric Drives, Power Electronics, Power Systems.



P. LAVANYA Received her B.Tech Degree from Sanketika Vidya Paishad, P.M.Palem, Visakhapatnam, Andhrapradesh and M.Tech from DADI Institute of Engineering & Technology, Anakapalle, Visakhapatnam, Andhrapradesh. She is currently working as Assistant

Professor in Department of EEE , GIITS Engineering College, Aganampudi, Visakhapatnam (Dt), Andhra Pradesh, India. Her area of Interest is Electric Drives.